Contribution from the Departments of Chemistry and Biochemistry and of Chemical Engineering and the Cooperative Institute for Research in Environmental Sciences, University of Colorado, Boulder, Colorado 80309, and Institute of Nuclear Energy and Technology, Tsinghua University, Beijing, China

Environmental Inorganic Chemistry. 1. Electrochemistry of a Water-Soluble Iron Porphyrin and Its Exploitation for Selective Removal and Concentration of Environmentally Hazardous Materials via Electrochemically Modulated Complexation

Carl A. Koval,*,† Steven M. Drew,† Richard D. Noble,† and Jianhan Yu‡

Received April 19, 1990

The electrochemistry and UV-vis spectroscopy of water-soluble iron tetrakis(*p*-sulfonatophenyl)porphyrin (Na_3[FeTPPS]) have been thoroughly investigated with respect to the interaction of Fe^{III}- and Fe^{II}TPPS with several nitrogen and sulfur donor ligands. On the basis of this information, a separation scheme for the selective removal and concentration of nitrogen heterocycles from a hydrocarbon solvent is demonstrated. This serves as a model for coal liquids polluted with polyaromatic heterocyclic compounds and illustrates the potential utilization of the process for removing environmentally hazardous materials from a variety of matrices. The process involves the use of electrochemistry to modulate the coordination of nitrogen heterocycles to FeTPPS, which serves as a carrier in a cyclic solvent extraction/release process. The modulation of the binding effectively changes the ability of an FeTPPS aqueous solution to extract and release various pollutants. The extensions of this process to other systems is also discussed.

Introduction

Iron porphyrins serve many functions in nature ranging from oxygen carriers in blood to catalytic centers in many proteins.[1] To date, many synthetic iron porphyrins have been synthesized and studied spectroscopically, magnetically, and electrochemically, creating a vast pool of knowledge on these structures.[2-4] A subset of this large group of compounds is the synthetic water-soluble iron porphyrins.[5,6] These compounds have also been intensely studied, not only for their relevance to biological systems but also because of their applications in electrocatalysis and magnetic resonance imaging.[7-9] Herein is reported the electrochemistry and application of iron tetrakis(*p*-sulfonatophenyl)porphyrin (FeTPPS) as an electroactive chemical complexing agent for a carrier-mediated separation scheme.

The electrochemistry of FeTPPS has been briefly described previously;[8,10] however, a complete study of the porphyrin has not been reported. Fe^{III}TPPS is known to exist as a monomer in acidic solutions and to dimerize to form a μ-oxo dimer ($[Fe^{III}TPPS]_2O$) in basic solutions;[6] the kinetics and mechanism of this dimerization process have been examined.[6,10,11] Reports have conflicted on the reduction products of $[Fe^{III}TPPS]_2O$.[8,12] One report stated evidence for the formation of a Fe^{II}TPPS dimer, while another report claimed that reduction of $[Fe^{III}TPPS]_2O$ produced two Fe^{II}TPPS monomers. Also, evidence for the formation of Fe^{I}TPPS has been given with no further characterization. This report completes the mechanistic picture of Fe^{III}TPPS electrochemistry.

The need for innovative separation technologies has been stated in a recent study by the National Research Council.[13] Developing reversible chemical complexing agents for the transport and concentration of solutes and improving the energy efficiency of separation techniques are generally considered high-priority research areas. One approach based on reversible chemical complexation is facilitated transport in liquid membranes.[14] This promising separation technique is based on a chemical carrier that is confined to a supported liquid membrane and selectively binds the solute to be separated. The carrier-solute complex diffuses across the liquid membrane where the equilibrium is reversed and the solute is released. The formation of the carrier-solute complex provides an additional pathway for the solute to cross the membrane, thus selectively increasing the total flux of the solute. Separations involving facilitated transport membranes have three important limitations: (1) the rate at which solutes can be removed is limited by the membrane surface area and the low diffusive mobility of the species within the liquid membrane; (2) a single carrier will not usually provide optimal transport for an entire class of permeates; (3) slow kinetics of the complexation reaction, especially the dissociation of the carrier-permeate complex, can greatly impair the effectiveness of a separation. Furthermore, the ability to increase the concentration of solutes during a separation process is highly desirable. This requires the introduction of an outside energy source to drive the solute concentration thermodynamically uphill. These aspects are all difficult or impossible problems to address within the context of facilitated transport.

The combination of electrochemistry and solvent extraction provides a means of addressing the limitations associated with facilitated transport in liquid membranes. Several accounts of electrochemically modulated complexation as applied to separation processes have appeared in the literature. One of the earliest reports by Ward described electrochemically induced carrier transport of NO by iron chloride confined in a liquid membrane.[15] Electrochemically switched binding of cations to crown ethers has also been described.[16] Accounts of the reaction of CO_2 with

† University of Colorado.
‡ Tsinghua University.

(1) (a) Cotton, F. A.; Wilkinson, G. *Advanced Inorganic Chemistry*, 5th ed.; John Wiley and Sons: New York, 1988; Chapter 30. (b) Smith, K. M., Ed. *Porphyrins and Metalloporphyrins*; Elsevier Scientific: Amsterdam, 1975.
(2) (a) Lever, A. B. P., Gray, H. B., Eds. *Iron Porphyrins: Part I*; Addison-Wesley: London, 1983. (b) Bertini, I.; Luchinat, C. *Paramagnetic Molecules in Biological Systems*; Benjamin-Cummings: Menlo Park, CA, 1986.
(3) Kadish, K. M. In *Iron Porphyrins: Part II*; Lever, A. B. P., Gray, H. B., Eds.; Addison-Wesley: London, 1983.
(4) Kadish, K. M. In *Progress in Inorganic Chemistry*; Lippard, S., Ed.; John Wiley and Sons: New York, 1986.
(5) Fleischer, E. B.; Palmer, J. M.; Srivastava, T. S.; Chatterjee, A. *J. Am. Chem. Soc.* **1971**, *93*, 3162-3167.
(6) Hambright, P.; Fleischer, E. B. *Inorg. Chem.* **1970**, *9*, 1757-1761.
(7) (a) Forshey, P. A.; Kuwana, T. *Inorg. Chem.* **1983**, *22*, 699-707. (b) Kline, M. A.; Barley, M. H.; Meyer, T. J. *Inorg. Chem.* **1987**, *26*, 2197-2198. (c) Barley, M. H.; Rhodes, M. R.; Meyer, T. J. *Inorg. Chem.* **1987**, *26*, 1746-1750.
(8) Barley, M. H.; Takeuchi, K. J.; Meyer, T. J. *J. Am. Chem. Soc.* **1986**, *108*, 5876-5885.
(9) Lauffer, R. B. *Chem. Rev.* **1987**, *87*, 901-927.
(10) Taniguchi, V. T. Ph.D. Dissertation, University of California, Irvine, 1978.
(11) Harris, F. L.; Toppen, D. L. *Inorg. Chem.* **1978**, *17*, 71-73.
(12) El-Awady, A. A.; Wilkins, P. C.; Wilkins, R. G. *Inorg. Chem.* **1985**, *24*, 2053-2057.
(13) National Research Council. *Separation and Purification: Critical Needs and Opportunities*; National Academy Press: Washington, DC, 1987.
(14) (a) Way, J. D.; Noble, R. D.; Flynn, T. A.; Sloan, E. D. *J. Membr. Sci.* **1982**, *12*, 239. (b) Way, J. D., Noble, R. D., Eds. *Liquid Membranes: Theory and Applications*; ACS Symposium Series 347; American Chemical Society: Washington, DC, 1987. (c) Noble, R. D.; Koval, C. A.; Pellegrino, J. *J. Chem. Eng. Prog.* **1989**, *85* (3), 58-70.
(15) Ward, W. J. *Nature* **1970**, *227*, 162-163.
(16) (a) Saji, T. *Chem. Lett.* **1986**, 275-276. (b) Echegoyen, L. E.; Yoo, H. K.; Gatto, V. J.; Gokel, G. W.; Echegoyen, L. *J. Am. Chem. Soc.* **1989**, *111*, 2440-2443.

0020-1669/90/1329-4708$02.50/0

various oxidation states of quinones[17,18] have appeared as a possible means of regenerative CO_2 removal for long-duration space missions.[18] Also, cobalt pentaamine complexes have been demonstrated to act as an electrochemically modulated carrier for the separation of oxygen from air and sea water.[19]

To demonstrate the effectiveness of this type of approach for separations, we have chosen to address the problem of removing environmentally hazardous compounds from low-grade petroleum fuels. These fuels are known to contain a variety of nonvolatile polyaromatic nitrogen and sulfur heterocycles.[20] Present technology requires high-pressure catalytic hydrogenation to reduce their levels. This process is expensive, requires large reactor and catalyst volumes, and is not specific. An alternative is to selectively remove the sulfur and nitrogen compounds and concentrate them in a hydrocarbon phase for subsequent treatment or disposal. $Fe^{II}TPPS$ reacts with many nitrogen and sulfur donor ligands in a reversible manner. However, these reactions have large equilibrium constants and the reaction is not easily reversed under equilibrium conditions. Electrochemistry provides a means of reversing these types of reactions. Oxidation of $Fe^{II}TPPS$ to $Fe^{III}TPPS$ under the appropriate solvent conditions drastically alters its affinity for a nitrogen or sulfur donor ligand. The modulation of the binding effectively changes the ability of an FeTPPS aqueous solution to extract and release various pollutants. This chemistry is used to set up an electrolysis/extraction system that selectively removes nitrogen-containing heterocycles from a "contaminated" hydrocarbon phase and then transports, releases, and concentrates them in another "waste" hydrocarbon phase.

Experimental Section

Reagents and Materials. The sodium salt of iron tetrakis(*p*-sulfonatophenyl)porphyrin ($Na_3[Fe^{III}TPPS]$) was synthesized by using a combination of literature methods.[6,10] $Na_3[Fe^{III}TPPS]$ was recovered as $Na_3[Fe^{III}TPPS]\cdot 9H_2O$ (fw = 1215.99), as shown by the elemental analysis. Anal. Calcd: C, 43.46; H, 3.49; N, 4.61; S, 10.55. Found: C, 43.44; H, 3.36; N, 4.33; S, 9.86. UV–visible spectrophotometry of $Na_3[Fe^{III}TPPS]$ at pH = 3 (1 mM $HClO_4$) and an ionic strength of 0.1 M ($NaClO_4$) gave the following results. Literature [λ, nm (ϵ, 10^4 cm^{-1} M^{-1})]: 392 (15.2), 528 (1.4), 680 (0.27).[6] Found [λ, nm (ϵ, 10^4 cm^{-1} M^{-1})]: 394 (15.7), 530 (1.32), 684 (0.266). Acridine (Aldrich), 1-aminoanthracene (Aldrich), 2-aminonaphthalene (Sigma), aniline (Aldrich), benzo[*b*]thiophene (Aldrich), carbazole (Aldrich), indole (Fisher), isoquinoline (Aldrich), methionine (Aldrich), methyl phenyl sulfide (Aldrich), pentamethylene sulfide (Aldrich), pyridine (Fisher), pyrrole (Aldrich), thiazole (Aldrich), and thiophene (Aldrich) were all at least 95% pure and were used as purchased. Buffers were made of citric acid, phthalic acid, phosphate, and boric acid depending on the pH required. The pH of the buffers was adjusted with NaOH or $HClO_4$, and the charge on the buffer was included in the ionic strength, *I*, calculation. $NaClO_4$ was the electrolyte in all cases. Isooctane (Aldrich) was used as a model coal liquid.

Instrumentation. Solution pH was measured with an Orion Research Model 701A digital Ionalyzer. Bulk electrolyses were conducted by using a PAR Model 371 potentiostat/galvanostat and a PAR Model 379 digital coulometer. Cyclic voltammetry was conducted by using either a Cypress System CYSY-1 or a PAR Model 363 potentiostat/galvanostat, a PAR Model 175 programmer, and an X-Y recorder. For the cyclic voltammograms (CV's) displayed here, cathodic current is positive and anodic current is negative. Working electrodes were either a highly polished Tokai glassy-carbon (GC) or a hanging-mercury-drop electrode (Metrohm AE290 HMDE). GC electrodes were polished with 0.5-μm alumina, rinsed thoroughly with distilled water, and then placed in a sonicator for 1 min to remove residual alumina from the surface of the electrode before each cyclic voltammogram was obtained. All potentials were measured versus the sodium chloride saturated calomel electrode (SSCE).

Table I. Molar Absorptivities of Pollutants in Isooctane

pollutant	λ, nm	ϵ, 10^3 M^{-1} cm^{-1}
acridine	358	7.9
1-aminoanthracene	390	3.9
2-aminonaphthalene	338	1.9
benzothiazole	286	1.5
benzo[*b*]thiophene	290	2.1
carbazole	234	4.7
isoquinoline	306	1.9
methyl phenyl sulfide	256	9.4
thiophene	232	15

The optically transparent thin-layer electrode (OTTLE) used was fabricated with quartz plates, 200 line/in. gold minigrid, and TEFZEL film. The cell construction is described elsewhere.[21] Thin-layer cyclic voltammograms were obtained with a PAR Model 173 potentiostat/galvanostat, a PAR Model 175 universal programmer, and an X-Y recorder. A PAR Model 179 digital coulometer was used for coulometric measurements. Spectra were obtained on a Hewlett-Packard HP8452A diode array UV–visible spectrophotometer run with HP89531A MS-DOS UV–vis operating software on a Zenith Z159 PC. Gas chromatography was performed by using a Hewlett-Packard HP5890 gas chromatograph on a HP-1 nonpolar capillary column.

Equilibrium Constant Measurements. The axial coordination of model ligands was investigated electrochemically to determine the extent of differential binding between $Fe^{III}TPPS$ and $Fe^{II}TPPS$. Shifts in $E_{1/2}$ upon the addition of ligand were related to equilibrium constants by combining the Nernst equation and the equilibrium expressions for ligand binding to each oxidation state of FeTPPS. These were rearranged to the form in eq 1,[3] where $(E_{1/2})_L$ is the $E_{1/2}$ of the CV for $Fe^{III}TPPS$

$$(E_{1/2})_L = E_{1/2} + RT/nF \ln [K_{Fe(II)}/K_{Fe(III)}] + (q - p)RT/nF \ln [L] \quad (1)$$

reduction in the presence of some concentration of ligand, [L]. $K_{Fe(II)}/K_{Fe(III)}$ is the ratio of equilibrium constants for the oxidation of $Fe^{II}TPPS$ to $Fe^{III}TPPS$, *p* is the number of ligands bound to $Fe^{III}TPPS$ (0, 1, or 2), and *q* is the number of ligands bound to $Fe^{II}TPPS$ (0, 1, or 2). The other constants have their usual significance. By titration of a solution of $Fe^{III}TPPS$ with a model ligand under the right conditions, the extent of differential binding between the two oxidation states can be determined along with the number of ligands bound in each oxidation state. The solution conditions were pH = 5.5 (phthalic acid buffer) and I = 0.1 M ($NaClO_4$).

The $K_{Fe(III)}$ for model ligands with $Fe^{III}TPPS$ was measured by using the method described in ref 27. A series of solutions were made of constant $Fe^{III}TPPS$ concentration and varying ligand concentration. The "limiting" spectrum was taken to be the pure ligated complex. The fraction, *f*, of the complex formed was calculated from the changes in absorbance at a specific wavelength: $f = (A - A_0)/(A_\infty - A_0)$, where A is the observed absorbance at some ligand concentration, A_0 is the absorbance of pure unligated $Fe^{III}TPPS$, and A_∞ is the absorbance of the pure complex. Combining *f* with the equilibrium expression leads to eq 2. Thus, a plot of log [L] versus log $[f/(1-f)]$ should give a slope equal

$$\log [f/(1-f)] = \log K_{Fe(III)} + p \log [L] \quad (2)$$

to the number of ligands bound to $Fe^{III}TPPS$ (0, 1, or 2) and a *y* intercept equal to log $K_{Fe(III)}$. The solution conditions were as follows: monomer, pH = 5.5 (phthalic acid buffer) and I = 0.1 (M $NaClO_4$); dimer, pH = 9.5 (boric acid buffer) and I = 1.0 M ($NaClO_4$).

(17) Mizen, M. B.; Wrighton, M. S. *J. Electrochem. Soc.* **1989**, *136*, 941–946.
(18) Bell, W. L.; Miedanner, A.; Smart, J. C.; DuBois, D. L.; Verostko, C. E. SAE tehnical Paper Series No. 881078; SAE: New York, 1988; pp 1–9.
(19) Ciccone, J. P.; Deardurff, L. A.; DeCastro, E. S.; Kerr, J. B.; Zenner, B. D. In *Redox Chemistry and Interfacial Behavior of Biological Molecules*; Dryhurst, G., Niki, K., Eds.; Plenum Press: New York, 1988; pp 397–406.
(20) Wilson, B. W.; Pelroy, R. A.; Mahlum, D. D.; Frazier, M. E.; Wright, C. W. In *Advanced Techniques in Synthetic Fuel Analysis*; Wright, C. W., Felix, W. D., Eds.; Technical Information Center, U.S. Department of Energy: Washington, DC, 1983; p 231.
(21) Drew, S. M.; Koval, C. A. Submitted for publication.
(22) Bard, A. J.; Faulkner, L. R. *Electrochemical Methods: Fundamentals and Applications*; John Wiley & Sons: New York, 1980.
(23) Kadish, K. M.; Larson, G.; Lexa, D.; Momenteau, M. *J. Am. Chem. Soc.* **1975**, *97*, 282–288.
(24) Dean, J. A., Ed. *Lange's Handbook of Chemistry*, 13th ed.; McGraw-Hill: New York, 1985.
(25) Fleischer, E. B.; Fine, D. A. *Inorg. Chim. Acta* **1978**, *29*, 267–271.
(26) (a) Gagne, R. R.; Allison, J. L.; Gall, R. S.; Koval, C. A. *J. Am. Chem. Soc.* **1977**, *99*, 7170–7178. (b) Allison, J. L. Ph.D. Dissertation, California Institute of Technology, 1979.
(27) Welnraub, D.; Peretz, P.; Faragi, M. *J. Phys. Chem.* **1982**, *86*, 1839–1842.

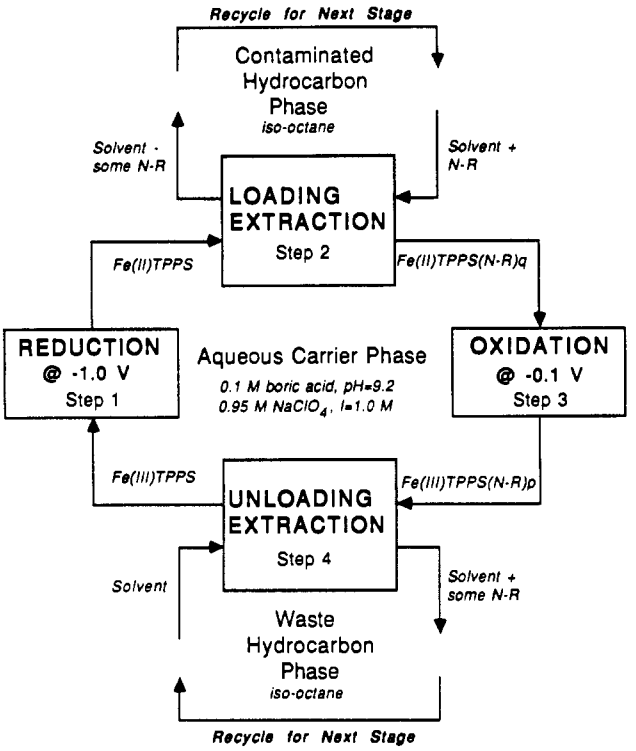

Figure 1. Block diagram of the staged extraction/electrolysis process showing the four steps that comprise one stage of the separation scheme.

Electrolysis/Extraction Procedure. Electrolyses for the procedure were performed in a two-compartment cell separated by a large surface area Nafion 117 membrane. Buffer solutions consisted of 0.1 M boric acid (pH = 9.2) and 0.95 M $NaClO_4$ (I = 1.0 M) in distilled deionized water. The working, reference, and auxiliary electrodes were a mercury pool, an SSCE, and a large platinum gauze, respectively. Electrolysis and extraction took place in a nitrogen-purged glovebox. Reductions of $Fe^{III}TPPS$ were done at −1.0 V, and oxidations were done at −0.1 V. For reduction the electrolysis was stopped when the current reached a steady state. This did not correspond to a stop in charge passed because of a fairly large background current. However, the current for the oxidation did decay to nearly zero, allowing exact determination of the end of electrolysis.

Effective distribution equilibrium constants (K_s, K_o, and K_r) were measured for the extraction of various pollutants from model coal liquids. K_s is the distribution equilibrium constant between the hydrocarbon and aqueous buffer phase (0.1 M boric acid, pH = 9.2; 0.95 M $NaClO_4$, I = 1.0 M), and K_o and K_r are the effective distribution equilibrium constants between the hydrocarbon phase and aqueous phase containing oxidized and reduced FeTPPS, respectively. The concentration of the pollutant in the hydrocarbon phase at equilibrium was determined by UV spectrophotometry. The calculated molar absorbtivities (ϵ) at the operating wavelength are shown in Table I. Indole and pentamethylene sulfide did not follow Beer's law and gave curved calibration curves. For K_r measurement, the extraction was conducted in the glovebox under N_2 atmosphere. When the reduction was completed, a given amount of reduced FeTPPS and hydrocarbon phase were taken into a separatory funnel and then shaken for about 2 min. The phases were then allowed to separate for about 5 min, and a sample was taken of the hydrocarbon phase. The concentration of the pollutant remaining in the hydrocarbon phase was determined, and K_r was calculated by using eq 3, where K_n

$$K_n = \{[N\text{-}R]_{o,i} - [N\text{-}R]_{o,e}\}V_o/[N\text{-}R]_{o,e}V_a \quad (3)$$

is K_s, K_o, or K_r, $[N\text{-}R]_{o,i}$ is the concentration of the pollutant initially in hydrocarbon phase, and $[N\text{-}R]_{o,e}$ is the concentration at equilibrium. V_o and V_a are the volumes of the hydrocarbon and aqueous phases, respectively. The measurement of K_s and K_o were made outside the glovebox in a similar fashion and calculated by using eq 3.

One stage of the electrolysis/extraction separation is outlined in Figure 1. The loading extraction procedure (step 2) was conducted as described for the K_r measurement following reduction of the FeTPPS aqueous phase (step 1). This hydrocarbon phase was called "contaminated", since it was meant to model a polluted coal liquid. After the loading extraction, the FeTPPS aqueous phase containing the extracted pollutant was oxidized (step 3). When the oxidation was finished, the aqueous phase was contacted with another hydrocarbon phase called the "waste" phase

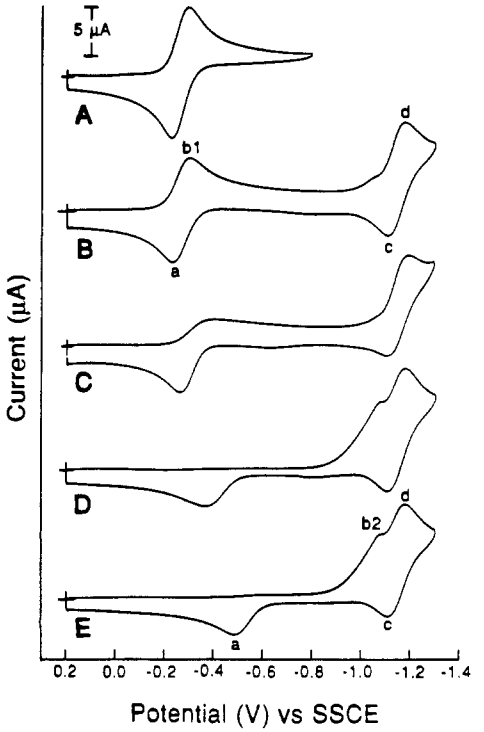

Figure 2. Cyclic voltammograms of FeTPPS at a glassy-carbon electrode and an ionic strength of 0.3 M as a function of pH: (A) $HClO_4$, pH = 2.5, 1.1 mM FeTPPS; (B) $NaClO_4$, pH = 4.6, 1.1 mM FeTPPS; (C) phthalic acid buffer, pH = 5.5, 1.0 mM FeTPPS; (D) boric acid buffer, pH = 10.0, 1.2 mM FeTPPS; (E) NaOH, pH = 12.1, 1.1 mM FeTPPS. The scan rate was 50 mV/s.

in an unloading extraction (step 4). This is the hydrocarbon phase in which the pollutants are to be concentrated. This extraction follows the procedure described for K_o measurement. The aqueous FeTPPS phase was again reduced in step 1 to begin another stage of the separation process. The initial volume ratio for the contaminated, waste, and aqueous phases was 4:1:1. Because of the crudeness of this process, it is impossible to maintain constant mass balance and a constant volume ratio. Therefore, care was taken to carefully record changes in these important values through several stages of electrolysis/extraction to allow model calculations based on K_s, K_o, and K_r to be performed.

Results and Discussion

Electrochemistry of FeTPPS. Effects of pH. Some cyclic voltammograms (CV's) of FeTPPS as a function of pH at a GC electrode are given in Figure 2. In acidic solutions, $Fe^{III}TPPS$ showed two reductions (see Figure 2A,B). This is similar to the CV's observed for the reduction of iron(III) tetraphenylporphyrin ($Fe^{III}TPP$) in nonaqueous solvents in this potential range.[3,4] In this case two consecutive metal-centered reductions to $Fe^{II}TPP$ and $Fe^{I}TPP$, respectively, were obtained.[3,4] Similarly, the consecutive reduction of $Fe^{III}TPPS$ to $Fe^{II}TPPS$ and $Fe^{I}TPPS$ has been shown here and elsewhere (see reactions 4 and 5).

$$Fe^{III}TPPS(H_2O)^{3-} + e^- + H_2O = Fe^{II}TPPS(H_2O)_2^{4-} \quad (4)$$

$$Fe^{II}TPPS(H_2O)_2^{4-} + e^- = Fe^{I}TPPS^{5-} + 2H_2O \quad (5)$$

As the pH was increased, the current for the first reductive wave, b1, was reduced and a new reductive wave, b2, appeared (Figure 2C–E). Also, once reductive wave b2 appeared, it did not change in peak potential (E_p). This is indicative of the formation of the more stable μ-oxo dimer, which has been well documented for both $Fe^{III}TPP$ and $Fe^{III}TPPS$.[3-5,10-12] $[Fe^{III}TPPS]_2O$ has been shown to be in equilibrium with $Fe^{III}TPPS(OH)(H_2O)$ in basic solution,[5,10-12] as seen in reaction 6. Variation

$$2Fe^{III}TPPS(H_2O)^{3-} = [Fe^{III}TPPS]_2O^{8-} + 2H^+ + H_2O \quad (6)$$

of the scan rate (v) from 0.005 to 5 V/s gave plots of $v^{1/2}$ versus peak current that were linear for waves a and b1 in both acidic and basic solutions. This indicates the lack of any surface adsorption.[22] The peak potential data for all CV's taken in the pH

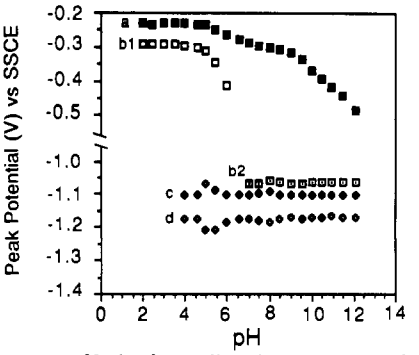

Figure 3. E_p versus pH plot for cyclic voltammograms of FeTPPS at a glassy-carbon electrode and an ionic strength of 0.3 M.

range 2–12 are summarized in Figure 3.

Several important facts can be ascertained from the E_p information presented in Figure 3. The half-wave potentials ($E_{1/2}$) for reactions 4 and 5 remained constant for pH = 2–5 and pH = 4–12, respectively. This indicates that no acid/base chemistry has taken place in those pH ranges for their respective half-reactions. For reaction 4, no acid/base chemistry is expected until the pH is near the pK_a for $Fe^{III}TPPS(H_2O)$ (pK_a = 6.5, I = 0.3 M).[12] Near pH = 6.5 the $Fe^{III}TPPS(H_2O)$ deprotonates; however, no shift in $E_{1/2}$ was detected because of reaction 6. The lack of shift in $E_{1/2}$ for reaction 5 indicates no ferrous hydroxy species were formed over the entire pH range studied. Also of interest is the constant E_p for the reduction of $[Fe^{III}TPPS]_2O$. Since there is no associated anodic current following reduction wave b2 and no evidence for the formation of ferrous hydroxy species, reaction 7 would be expected. However, this reaction seems to contradict

$$[Fe^{III}TPPS]_2O^{8-} + 2e^- + 2H^+ + 3H_2O = 2Fe^{II}TPPS(H_2O)_2^{4-} \quad (7)$$

the fact that no pH dependence was observed for the position of wave b2. In the case of $[Fe^{III}TPP]_2O$ reduction in nonaqueous solvents, it has been shown that the intermediate mixed-valence dimer $Fe^{II}TPP$–O–$Fe^{III}TPP$ has transient stability.[23] The instability of $Fe^{II}TPP$–O–$Fe^{III}TPP$ leads to a formal potential ($E^{\circ\prime}$) for its reduction that is much less than the $E^{\circ\prime}$ for the first reductive step.[23] The same mechanism could be expected for $[Fe^{III}TPPS]_2O$ reduction, as seen in reactions 8 and 9. Reaction

$$[Fe^{III}TPPS]_2O^{8-} + e^- = Fe^{II}TPPS\text{–}O\text{–}Fe^{III}TPPS^{9-} \quad E_8^{\circ\prime} \quad (8)$$

$$Fe^{II}TPPS\text{–}O\text{–}Fe^{III}TPPS^{9-} + e^- + 2H^+ + 3H_2O = 2Fe^{II}TPPS(H_2O)_2^{4-} \quad E_9^{\circ\prime} \ll E_8^{\circ\prime} \quad (9)$$

9 is now the pH-dependent reduction, and since $E_9^{\circ\prime} \ll E_8^{\circ\prime}$, any shift in $E_9^{\circ\prime}$ would not be detected by a shift in the E_p for wave b2.

Cyclic voltammograms at different pH values were also recorded with an HMDE. These CV's showed $E_{1/2}$'s and heterogeneous kinetics similar to those recorded at GC electrodes in acidic solutions. However, in basic solutions, the magnitude of the currents associated with wave a were greatly reduced.

Thin-Layer Spectroelectrochemistry. Thin-layer spectroelectrochemistry was performed to determine the spectra of reduced $Fe^{III}TPPS$ in both acidic and basic solutions (see Figure 4) and confirm the number of electrons, n, for reactions 4, 5, and 7 by exhaustive electrolysis. Reaction 4 was found to have n = 1.04 ± 0.04 (2.02 mM FeTPPS, pH ~ 4, I = 0.3 M), for reduction at −0.5 V vs SSCE. Unfortunately, n for reaction 5 and the spectrum of $Fe^{I}TPPS$ could not be determined due to the formation of bubbles in the OTTLE when it was poised at very negative potentials (~1.3 V vs SSCE). For reaction 7, an n = 1.8 ± 0.2 (1.03 mM $[Fe^{III}TPPS]_2O$, pH = 9.5, I = 1.0 M) was measured for reduction of $[Fe^{III}TPPS]_2O$ at −1.0 V vs SSCE.

The spectra in Figure 4 and thin-layer electrolysis data above confirm the mechanism of $Fe^{III}TPPS(H_2O)$ and $[Fe^{III}TPPS]_2O$ reduction surmised from the CV data and some literature reports.[8] The reduction of $Fe^{III}TPPS(H_2O)$ to $Fe^{II}TPPS(H_2O)_2$ is one-electron, and the $[Fe^{III}TPPS]_2O$ dimer undergoes a two-electron reduction followed by immediately cleavage to two $Fe^{II}TPPS(H_2O)_2$ monomers.

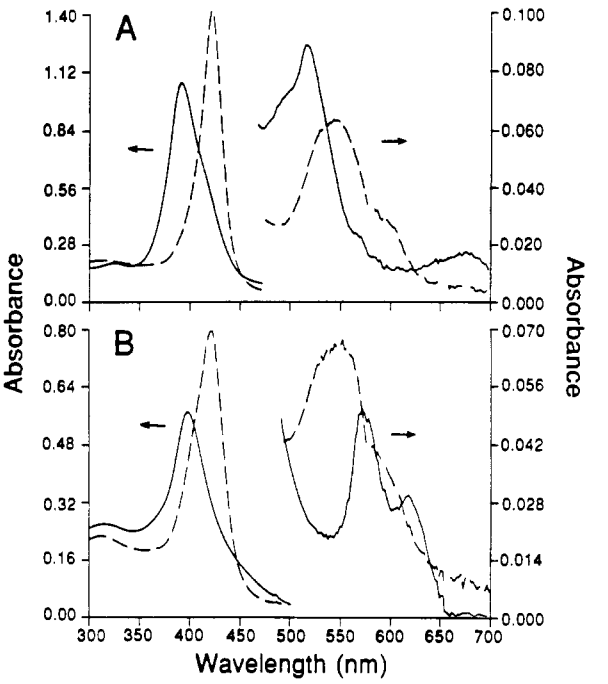

Figure 4. Thin-layer spectra of FeTPPS under various conditions of pH and ionic strength: (solid lines) $Fe^{III}TPPS$ spectra; (dashed lines) $Fe^{II}TPPS$ spectra; (A) $NaClO_4$, pH = 4, I = 0.3 M, 2.0 mM FeTPPS; (B) boric acid buffer, pH = 9.5, I = 1.0 M, 2.0 mM FeTPPS.

Table II. FeTPPS Thin-Layer Spectroelectrochemistry Results

porphyrin and conditions	λ, nm	ε, 10^4 cm^{-1} M^{-1}
$Fe^{III}TPPS(H_2O)_3^-$	394	15
2.03 mM	528	1.3
pH ~ 4, I = 0.3 M[a]	680	0.23
$Fe^{II}TPPS(H_2O)_2^{4-}$	426	20
2.03 mM	556	0.91
pH ~ 4, I = 0.3 M	594	0.45
$[Fe^{III}TPPS]_2O^{8-}$	402	17
1.00 mM	580	1.5
pH = 9.5, I = 1.0 M[b]	624	0.91
$Fe^{II}TPPS(H_2O)_2^{4-}$	426	12
2.01 mM	556	0.92
pH = 9.5, I = 1.0 M	594	0.55

[a] Unbuffered solution of $NaClO_4$. [b] 0.1 M boric acid buffer, 0.95 M $NaClO_4$.

All the spectral data obtained in these thin-layer spectroelectrochemical experiments are summarized in Table II. The spectra of $Fe^{III}TPPS(H_2O)$ and $Fe^{II}TPPS(H_2O)_2$ recorded in low ionic strength solutions (I = 0.3 M) agree well with the literature.[5,8,10] However, the spectra of $[Fe^{III}TPPS]_2O$ and $Fe^{II}TPPS(H_2O)_2$ in high ionic strength solution (I = 1.0 M) show some differences. For $[Fe^{III}TPPS]_2O$ another spectrum was obtained at lower concentration (10 μM $[Fe^{III}TPPS]_2O$, pH = 9.5, I = 1.0 M) in a conventional quartz cell under conditions similar to those used in the literature. In this case, the spectrum was found to change to the wavelengths previously reported[5] [found [λ, nm (ε, 10^4 cm^{-1} M^{-1})]: 408 (22), 568 (1.7), 608 (0.27)]. The spectrum of $Fe^{II}TPPS(H_2O)_2$ in basic, high ionic strength solutions showed a significant decrease in the intensity of its Soret band. Since the same effect is observed in acidic solutions of high ionic strength (I = 1.0 M), this is not believed to be caused by the change in pH but by the higher ionic strength.

Axial Ligand Binding to FeTPPS. The reaction of nitrogen and sulfur donor ligands with FeTPP in nonaqueous solvents has been well documented.[3,4] Both spectral and electrochemical methods have been shown to be useful.[2-4] The interest here is in the examination of the coordination of nitrogen and sulfur

Table III. Classes of Pollutants Found in Coal Liquids and Proposed Model Ligands

chemical classes of pollutants	model ligand	chemical classes of pollutants	model ligand
polyaromatic amines	aniline	polyaromatic sulfur heterocycle	thiophene
secondary polyaromatic nitrogen heterocycles	pyrrole	thioether	methionine
tertiary polyaromatic nitrogen heterocycles	pyridine	polyaromatic mixed heterocycles	thiazole

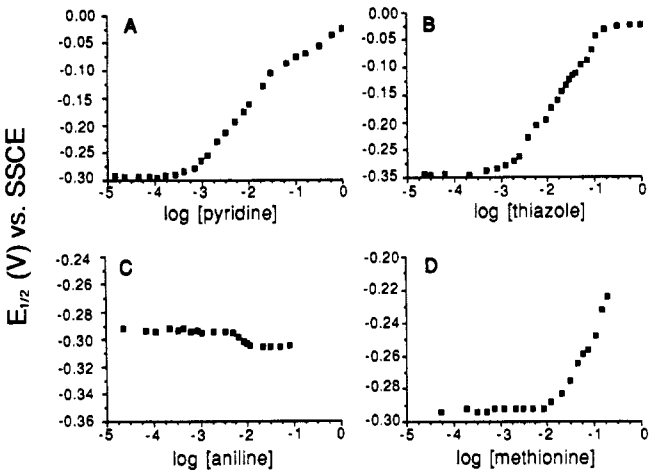

Figure 5. $E_{1/2}$ for FeTPPS as a function of ligand concentration: (A) pyridine; (B) thiazole; (C) aniline; (D) methionine. Solution conditions were pH = 5.5 (phthalic acid buffer) and I = 0.1 ($NaClO_4$). The scan rate was 50 mV/s.

heterocycles (pollutants) to FeTPPS in aqueous solution. Working in water poses several complications that include the low solubility of large nitrogen and sulfur heterocycles in aqueous solution and the possibility of ligand protonation in acidic solution. To solve the problem of low solubility, the coordination chemistry of small model ligands has been investigated. As seen in Table III, each small ligand chosen to model a specific pollutant class[20] is known to have a fairly high solubility in water or ethanol–water mixtures.[24]

Of the six model ligands studied, only two were found to have no coordination chemistry with FeTPPS. They were thiophene and pyrrole. Both of these ligands showed no shift in $E_{1/2}$ up to 0.1 M ligand.

Additions of pyridine to a solution of FeTPPS produced definite shifts in $E_{1/2}$, as seen in Figure 5A. $E_{1/2}$ was constant (−0.293 V), then began to shift positive with a slope of about 0.10 V (q = 2, p = 0), and then leveled off at about 0.1 M pyridine (q = 2, p = 2). At this point the $E_{1/2}$ began to shift positive again; however, this was most likely due to the large increases in ionic strength that occurred at high pyridine concentrations (pH of experiment was 5.5, and pyridine has a pK_a of 5.2[24]). If the $E_{1/2}$ at 0.1 M pyridine (−0.075 V) is estimated to be approximately equal to the true $E_{1/2}$ at 1 M pyridine (excluding increased dimerization of $Fe^{II}TPPS$), then $K_{Fe(II)}/K_{Fe(III)}$ is 5×10^3 when q and p are 2. $K_{Fe(III)}$ has been measured previously to be 1.5×10^3.[25] From these data, an approximate $K_{Fe(II)}$ of 8×10^6 was calculated.

Thiazole also showed a definite reaction with FeTPPS. As seen in Figure 5B, an $E_{1/2}$ vs log [L] curve similar to that of pyridine was obtained. This implies that thiazole coordinates to FeTPPS through the nitrogen heteroatom rather than the sulfur. The region between −3 and −1 log [thiazole] gave a slope of 0.11 V (q = 2, p = 0), which leveled off to a steady $E_{1/2}$ value of −0.024 V (q = 2, p = 2). From this $E_{1/2}$ the ratio $K_{Fe(II)}/K_{Fe(III)}$ is calculated to be 4×10^4. For thiazole, a plot of log [thiazole] versus log $[f/(1-f)]$ yielded a slope of 1.8 (p = 2) and a y intercept of 2.2 ($K_{Fe(III)} = 1 \times 10^2$). This resulted in the calculated $K_{Fe(II)}$ being about 5×10^6. The spectroscopic parameters found for $Fe^{III}TPPS(thiazole)_2$ were as follows [λ, nm (ε, 10^4 cm^{-1} M^{-1})]: 416 (14), 542 (0.89).

Table IV. Equilibrium Constants Measured for FeTPPS + Model Ligands

form	pH range	methionine[b,c]	pyridine[a,c]	thiazole[b,c]	aniline[b,c]
$Fe^{III}TPPS$ monomer	4.0–5.8	2×10^3	1×10^2	5×10^4	$<10^{-7}$
$Fe^{III}TPPS$ dimer	>8.7	$<10^{-7}$	$<10^{-7}$	$<10^{-7}$	$<10^{-7}$
$Fe^{II}TPPS$ monomer	5.5	7×10^6	5×10^6	3×10^4	5×10

[a] $Fe^{III}TPPS + 2L = Fe^{III}(TPPS)L_2$; [FeTPPS] = 10^{-6} M, μ = 0.1 M; taken from ref 27. [b] $Fe^{III}TPPS + 2L = Fe^{III}(TPPS)L_2$; [FeTPPS] = 10^{-4} M, μ = 0.1 M; this work. [c] $Fe^{II}TPPS + 2L = Fe^{II}(TPPS)L_2$, for L = pyridine, thiazole, and aniline; $Fe^{II}TPPS + L = Fe^{II}(TPPS)L$, for L = methionine; [FeTPPS] = 10^{-3} M, μ = 0.1 M; this work.

Aniline reacted with FeTPPS in a much different way, as seen in Figure 5C. Addition of aniline to a solution of $Fe^{III}TPPS$ gave a negative shift in $E_{1/2}$ instead of a positive one. This indicates that $K_{Fe(III)}$ must be greater than $K_{Fe(II)}$. The $E_{1/2}$ shifted from −0.293 to −0.304 V, implying that $K_{Fe(II)}/K_{Fe(III)}$ = 0.6 and p must equal q. Results of the spectroscopic determination of $K_{Fe(III)}$ were a slope of 2.0 (p = 2.0) and a y intercept of 4.7 ($K_{Fe(III)} = 5 \times 10^4$). $K_{Fe(II)}$ was calculated to be 3×10^4. The spectroscopic parameters found for $Fe^{III}TPPS(aniline)_2$ were as follows [λ, nm (ε, 10^4 cm^{-1} M^{-1})]: 418 (16), 546 (1.0), 628 (0.11).

Methionine showed a positive shift in $E_{1/2}$ at a relatively high concentration of ligand (see Figure 5D). The slope of the shifted region was found to be 0.060 V (q = 1 or 2, p = 0 or 1). Investigation into the coordination of methionine to $Fe^{III}TPPS$ showed no visible spectroscopic changes up to a concentration of ligand 10^3 times greater than the $Fe^{III}TPPS$ concentration. Thus, it was concluded that $Fe^{III}TPPS$ does not react with methionine at any reasonable concentration and that q must be 1 and p is 0. $K_{Fe(II)}$ was determined by using a simplified version of eq 8 for small equilibrium constants where only one ligand is bound to one oxidation state[26] (see eq 10). From eq 10, an average $K_{Fe(II)}$ of 5×10 was calculated.

$$(E_{1/2})_L = E_{1/2} + RT/nF \ln \{1 + K_{Fe(II)}[L]\} \qquad (10)$$

The results of all the equilibrium constant measurements are summarized in Table IV. On the basis of these results, tertiary nitrogen heterocycles and some mixed heterocycles would be expected to have the most favorable differences in $K_{Fe(III)}$ and $K_{Fe(II)}$. Polyaromatic amines and thioethers should display little difference between $K_{Fe(III)}$ and $K_{Fe(II)}$ and small equilibrium constants, respectively. However, it has been previously observed that dimerization of $Fe^{III}TPPS$ greatly reduces its affinity for nitrogen donor ligands.[25,27] As seen in Table IV, the reaction of $[Fe^{III}TPPS]_2O$ in basic aqueous solutions with the model pollutants could not be observed ($K_{Fe(III)} < 10^{-7}$). However, $K_{FE(II)}$ would be expected to remain about the same, since no evidence of ferrous hydroxy formation could be detected in the pH range studied. Thus, to create an electrochemically modulated binding cycle in which one oxidation state has no affinity for a pollutant, it would be advantageous to use basic conditions, i.e. pH = 9.5 (boric acid buffer) and I = 1.0 M ($NaClO_4$), under which $Fe^{III}TPPS$ is dimerized to $[Fe^{III}TPPS]_2O$.

FeTPPS Extraction/Electrolysis Process. K_s, K_o, and K_r Determinations. K_s, K_o, and K_r were determined as described in the Experimental Section and are listed in Table V. Trends in the distribution equilibrium constants were generally as predicted by FeTPPS binding experiments with small model ligands. Derivatives of pyrrole such as indole and carbazole showed only small differences between K_o and K_r. For benzo[*b*]thiophene and thiophene, a low K_s (i.e. low physical solubility) was found. In this case, reaction with FeTPPS would not be expected. For thioethers such as pentamethylene sulfide and methyl phenyl sulfide, the low K_s precluded the expected FeTPPS reaction. The best results were obtained for the tertiary nitrogen heterocycles and the polyaromatic amines. In both these cases significant increases in K_r relative to K_o were found. Compounds such as

Table V. Distribution Equilibrium Constants

pollutants	binding[a]	K_s[b]	K_o[c]	K_r[d]
acridine	yes[e]	0.026	0.020	1.6 (0.055)[h]
1-aminoanthracene	yes[e]	0.035	0.28	2.1 (0.061)
2-aminonaphthalene	yes[e]	0.087	0.56	3.0 (0.060)
benzothiazole	yes[g]	0.056	0.15	0.41 (0.72)
benzo[*b*]thiophene	no[f]	<0.0002[i]	<0.0002	<0.0002
carbazole	no[f]	0.056	0.13	0.12 (0.61)
indole	no[f]	0.13	0.37	0.37 (0.50)
isoquinoline	yes[g]	0.12	0.48	15 (0.12)
methyl phenyl sulfide	yes[f]	<0.0002[i]	<0.0002	<0.0002
pentamethylene sulfide	yes[f]	~0.004	~0.004	~0.004
thiophene	no[f]	~0.01	~0.01	~0.01

[a] Indicates if any axial binding would be expected on the basis of cyclic voltammetry experiments. [b] 0.1 M boric acid buffer (pH = 9.2), 0.95 M $NaClO_4$ (I = 1.0 M). [c] 0.1 M boric acid buffer (pH = 9.2), 0.95 M $NaClO_4$ (I = 1.0 M), 10 mM $Fe^{III}TPPS$. [d] 0.1 M boric acid buffer (pH = 9.2), 0.95 M $NaClO_4$ (I = 1.0 M), 10 mM $Fe^{III}TPPS$ reduced at −1.0 V vs SSCE. [e] Compounds were too insoluble for direct determination of any axial binding in water; thus, estimates based on cyclic voltammetry binding experiments with soluble analogues are shown here. [f] 50% ethanol, 1 mM $HClO_4$, 0.1 M $NaClO_4$ (I = 0.1 M). [g] 0.02 M phthalic acid (pH = 5.5), 0.06 M $NaClO_4$ (I = 0.1 M). [h] Concentration (mM) of the compound in the hydrocarbon phase at equilibrium. [i] Equilibrium constant too small to measure.

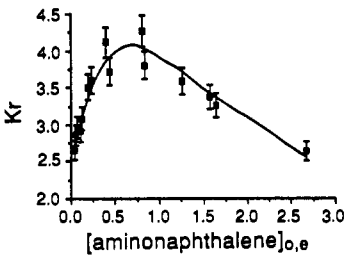

Figure 6. Dependence of K_r on the concentration of 2-aminonaphthalene in the organic phase at equilibrium. Solid line indicates mathematical fit to data.

2-aminonaphthalene and isoquinoline had sufficiently high K_s's to allow reactions with FeTPPS to occur.

The values of K_s and K_o were found not to change significantly with the concentration of the pollutant in the organic phase at equilibrium, $[N\text{–}R]_{o,e}$. However, K_r showed marked differences depending on $[N\text{–}R]_{o,e}$. This is why values of $[N\text{–}R]_{o,e}$ are given along with K_r in Table V. K_r dependence for 2-aminonaphthalene (ANP) is illustrated in Figure 6. As the $[N\text{–}R]_{o,e}$ of ANP increased, K_r increased to a maximum of about 4 at 0.6 mM ANP and then steadily decreased. Modeling studies of these types of curves can provide information on the binding equilibrium, the number of pollutants bound, and the aggregated state of the reduced porphyrin.[28] For example, the solid line in Figure 6 is obtained by assuming a $K_{Fe(II),1}$ (one to one reaction) of 7×10^3, a $K_{Fe(II),2}$ (one to two reaction) of 2×10^4, and a concentration of $Fe^{II}TPPS$ of 4 mM (total $Fe^{II}TPPS$ concentration was about 8 mM). These reaction parameters imply the formation of an $Fe^{II}TPPS$ aggregate dimer that favors axial coordination of two 2-aminonaphthalenes.[28]

K_r also showed a strong dependence on the total concentration of the carrier (C_T) present in solution. This is demonstrated for isoquinoline (ISQ) extraction in Figure 7. In this case, the feed concentration of ISQ for the series of extractions was held constant; thus the $[N\text{–}R]_o$ for ISQ decreases with increasing C_T. As C_T was increased, K_r increased at a much faster rate than K_o, indicating that large concentrations of FeTPPS will give the most efficient extractions.

Single- and Multiple-Component Staged Separations. Staged separations were performed as described in the Experimental Section. On the basis of the data in Table V, three pollutants were selected to demonstrate the staged electrolysis/extraction process. The pollutants were ISQ, ANP, and indole (IND). These three pollutants have similar K_s and K_o values but have significantly different K_r values (see Table V). The results of the single-component staged separation experiments are shown in Figure 8. ISQ gave the best results, demonstrating that the staged electrolysis/extraction process can remove 1.1 mM ISQ from a contaminated phase down to about 0.086 mM and concentrate it in a waste phase to about 2.8 mM (see Table VI). Results for ANP showed less concentrating power, as predicted by its smaller K_r, and IND was not concentrated at all since it had no reaction with FeTPPS.

The results for IND (see Figure 8C) represent what would be expected for a normal solvent extraction process, i.e. one that does not involve electrochemically modulated complexation. The concentrations of IND in the contaminated and waste phases asymptotically approach each other and would become equal after additional stages of the process. The final equilibrium concentration in the waste phase did not equal half of the initial concentration in the contaminated phase because the approximate volume ratio was 4:1 (contaminated phase:waste phase). The only observed effect of FeTPPS on the removal and concentration of IND is the small increase in K_r and K_o over K_s (see Table V). In this case, FeTPPS was acting as a modifier that slightly increased the physical solubility of IND in the aqueous phase.

The results for ISQ and ANP (see Figure 8A,B) are substantially different from those obtained for IND and demonstrate the advantages of electrochemically modulated complexation. The relatively large values of K_r caused by complexation to $Fe^{II}TPPS$ result in rapid removal from the contaminated organic phase. As seen in Figure 8A, equilibrium levels of ISQ are approached after only two stages. In both cases, the concentrations in the waste phase after four stages exceed the initial concentrations in the

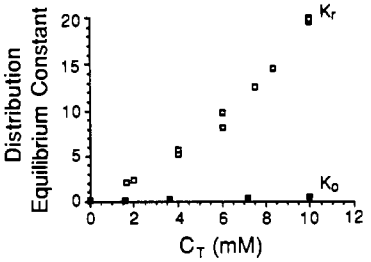

Figure 7. Dependence of K_r (open squares) and K_o (closed squares) on the total concentration of FeTPPS in the aqueous phase for isoquinoline extraction.

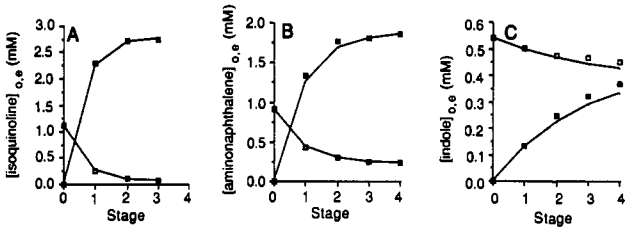

Figure 8. Single-component staged electrolysis/extraction process for the separation of a pollutant from a contaminated phase (open squares) into a waste phase (closed squares): (A) isoquinoline; (B) 2-aminonaphthalene; (C) indole. Solid lines indicate results of mass balance calculations.

Table VI. Staged Electrolysis/Extraction Results for Isoquinoline

	contaminated phase		waste phase		aqueous phase	
stage	[ISQ], mM	V, mL	[ISQ], mM	V, mL	[ISQ], mM	V, mL
0	1.11	48	0	12	0	12
1	0.26	48	2.3	12	1.2	11.5
2	0.11	45	2.7	11	1.3	11.5
3	0.086	42	2.8	10	1.4	11.5

(28) Jianhan, Y.; Drew, S. M.; Noble, R. D.; Koval, C. A. Manuscript in preparation.

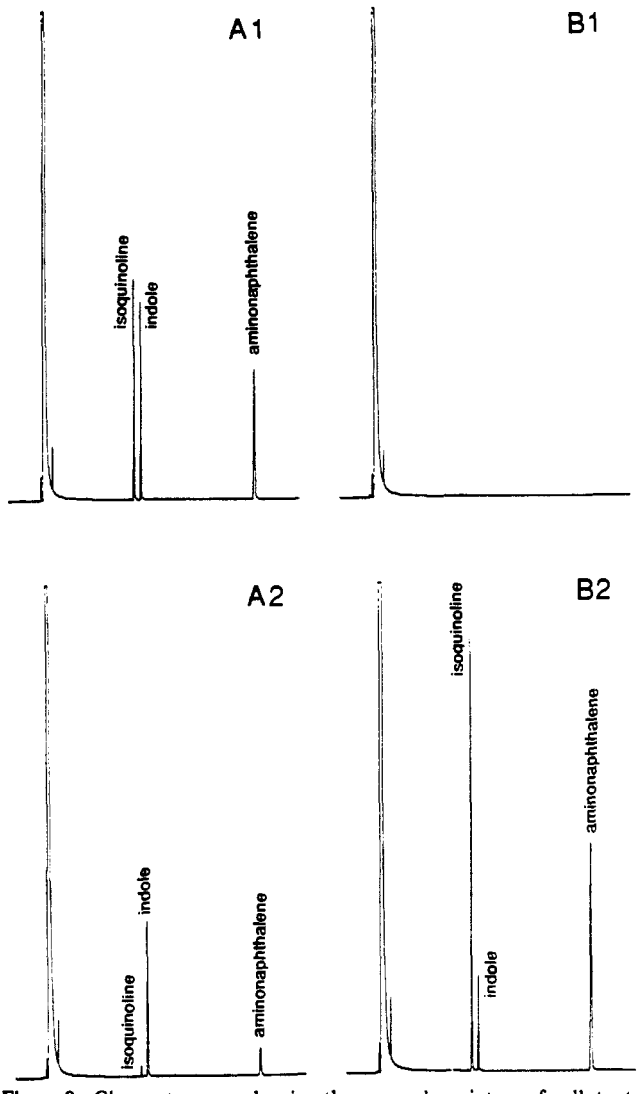

Figure 9. Chromatograms showing the removal a mixture of pollutants from a contaminated phase and concentration into a waste phase: (A1) contaminated phase before extraction; (A2) contaminated phase after extraction; (B1) waste phase before extraction; (B2) waste phase after extraction.

contaminated phase. The energy for this increase in concentration comes from the electrochemical oxidation of the $Fe^{II}TPPS$ complex to $[Fe^{III}TPPS]_2O$, which has little affinity for ISQ and ANP. The removal and concentration effect is better for ISQ than for ANP because of the greater difference in K_o and K_r for ISQ.

The results are entirely consistent with the results of mass balance calculations performed at each stage in the process. The results for such calculations are represented by the solid lines in Figure 8. The actual data for ISQ given in Table VI show the loss of solution that occurs during the experimental procedure. These changes in solution volume were carefully recorded to determine the mass balance calculation at each stage. A complete mathematical analysis describing equilibrium stage processes will be published elsewhere.[29] For given values of K_o and K_r, the analysis allows ready calculation of the concentration in each phase at every stage and predicts the number of stages required to reach final equilibrium.[29]

A mixture of the three pollutants used above was employed to demonstrate a staged separation of a simulated polluted coal liquid. The gas chromatograms of the respective solutions before and after the electrolysis/extraction process are shown in Figure 9. They show the marked decrease in ISQ and ANP concentrations expected on the basis of the single-component staged separations. Again, the results are consistent with mass balance calculations[29] and there is little "competition" of the pollutants for the FeTPPS carrier. This is because the initial concentration of the pollutants ($\sim$1 mM) is small compared to the FeTPPS concentration ($\sim$10 mM). If larger concentrations of pollutants or larger volumes of the contaminated phase were used, competition effects would be significant.

Conclusions and Future Directions

The electrochemistry and UV–vis spectroscopy of water-soluble iron tetrakis(*p*-sulfonatophenyl)porphyrin (Na_3[FeTPPS]) have been thoroughly investigated with respect to the interaction of Fe^{III}- and $Fe^{II}TPPS$ with several nitrogen and sulfur donor ligands. On the basis of this information, a separation scheme has been designed and demonstrated for the selective removal of nitrogen heterocycles from a hydrocarbon solvent that serves as a model coal liquid polluted with polyaromatic heterocyclic compounds. The process involved the use of electrochemistry to modulate the coordination of nitrogen heterocycles to FeTPPS, which served as a carrier molecule. The modulation of the binding effectively changed the ability of an FeTPPS aqueous solution to extract and release various pollutants. The effectiveness of this process was demonstrated via a selective solvent extraction method for single- and multiple-component solutions.

This study indicates that electrochemically modulated complexation can be used to improve the performance of extraction-based separation processes. Two key features are demonstrated. First, the redox and complexation reactions associated with the carrier are shown to operate in a reversible chemical cycle. Second, electrical energy is utilized to increase the concentration of solutes as part of the separation process. It appears that the process described herein could be extended to numerous separation problems that currently exist in processing industries and in attempts to remove hazardous chemicals from the environment. Most aspects of the electrochemically modulated complexation process are amenable to scale-up in a manner analogous to other extraction processes, indicating that large quantities of polluted liquid phases could be treated. The theoretical energy requirements for electrochemical concentration of solutes are lower that those for heat-driven concentration methods, such as distillation and evaporation. Achieving these theoretical limits will require improvements in the voltage swing required to modulate the complexation reaction.

Acknowledgment. This work was supported under National Science Foundation Grant No. CBT 8813036 and Pittsburgh Energy Technology Center (Department of Energy) Grant No. DE-PS22-88PC89999.

(29) Jianhan, Y.; Jeema, N.; Noble, R. D.; Koval, C. A. Submitted for publication.